Pergamon

*Int. J. Multiphase Flow* Vol. 22, No. 6, pp. 1205–1222, 1996

PII: S0301-9322(96)00035-3
0301-9322/96 $15.00 + 0.00

# INFILTRATION OF INITIALLY DRY, DEFORMABLE POROUS MEDIA

L. PREZIOSI[1], D. D. JOSEPH[2] and G. S. BEAVERS[2]

[1]Dipartimento di Matematica, Politecnico, Corso Duca degli Abruzzi 24, Torino, 10129, Italy
[2]Department of Aerospace Engineering and Mechanics, University of Minnesota, 110 Union St. SE, Minneapolis, MN 55455, U.S.A.

*(Received 14 November 1995; in revised form 6 May 1996)*

**Abstract**—The present paper studies the infiltration of an incompressible liquid in an initially dry (or partially dry), deformable sponge-like material made of an incompressible constituent in the slug-flow approximation having in mind the application to some industrial processes involving flow through sponge-like materials and, in particular, some composite materials manufacturing processes. The resulting initial-boundary value problem is of Stefan type, with suitable interface conditions and evolution equations describing the position of the interfaces delimiting the saturated region within the porous material. Different models are then suggested in the saturated region, depending on the importance of the inertial terms and on the constitutive equation for the stress. Comparison of the simulation with known experimental results is satisfactory. Copyright © 1996 Elsevier Science Ltd.

*Key Words:* deformable porous media, composites manufacturing

## 1. INTRODUCTION

Many manufacturing processes used to fabricate composite materials involve injecting a metallic, ceramic or polymeric melt into a deformable porous material. This solid preform can be made of a sponge-like material, or of a solid constituent in the form of mats, fibers, whiskers, particulates, flakes, or wires (see, for example, Christensen 1979; Cook 1977; Gibson 1994; Isayev 1987; Macosko 1989; and Mallick 1988).

After solidification of the melt, the reinforcing network within the composite material carries the major stresses and loads, while the solidified matrix material holds the reinforcing elements together, enabling the transfer of the stresses and loads to them.

These manufacturing processes, usually referred to as resin transfer molding (RTM), structural resin injection molding (SRIM), and squeeze casting, can be schematized as infiltration problems in initially dry porous media. In modelling them in the literature it is usually assumed that the solid preform is rigid, in spite of the fact that several papers show or describe qualitatively deformation of the solid constituent and emphasize the importance of monitoring the dynamical evolution of the deformation and stress states to identify in advance possible inhomogeneities and damages in the reinforcing network (see Gonzalez-Romero & Macosko 1990; Han *et al.* 1993a, b; Kim *et al.*, 1991; Lacoste *et al.* 1991, 1993; Mortensen & Wong 1990; Rudd *et al.* 1990, 1992; Sommer & Mortensen 1996; Trevino *et al.* 1991; Yamauchi & Nishida 1995; Young *et al.* 1991a; and Preziosi 1996 for a recent review on the subject).

Furthermore, from the industrial point of view there is a crucial need to identify a good compromise between rate of production and quality of the product, such as, for example, obtaining a homogeneous composite material, and avoiding ruptures of the reinforcing fibers which can lead to material failures. This requires a detailed description of the whole dynamics of the coupling between the flow and the deformation of the porous material.

When a fluid flows through a deformable porous medium the forces associated with the flow deform the porous material. In turn, the deformation of the porous medium influences the flow. The competition among the stress in the solid element, pressure in the liquid element and inertial and body forces will determine the evolution of the system, which is very different from that experimentally observed when the coupling between fluid flow and deformation of the porous

medium is absent. In fact, the strain distribution in a deformable porous medium is uniform if it is subjected to a steady mechanical compression and highly nonuniform if the strain is produced by fluid flow (see, for instance, figure 1 of Parker *et al.* 1987).

Similar coupled flow/deformation problems have been studied in several different scientific fields: in soil mechanics (see, for instance, Barenblatt *et al.* 1990; Bear & Bachmat 1990; Lee *et al.* 1983; Lancellotta 1995, and references therein), in magma mechanics (Fowler 1985; Richter & McKenzie 1984; Scott *et al.* 1984, 1986, 1988; Spiegelman 1993a, b), in bio-mathematics (Barry & Aldis 1991; Holmes & Mow 1990; Kenyon 1976, 1979; Kwan *et al.* 1990; Lai *et al.* 1981, 1990; Mow *et al.* 1979, 1980, 1984; Oomens *et al.* 1987; Sorek & Sideman 1986, and references therein), and in dealing with several industrial processes such as paper pulp rolling, fabric dyeing and drying, coffee brewing, and so on (see, Fasano *et al.* 1992, 1993; Lord 1955; and Taub 1967).

Having in mind the application to those industrial processes involving flow through sponge-like materials and, in particular, injection molding and squeeze casting processes, we study in this paper the problem of the spontaneous relaxation of a compressed wet sponge and the infiltration of an incompressible liquid into an initially dry (or partially dry) deformable sponge-like material made from an incompressible solid in the slug-flow approximation.

This assumption, which is acceptable when the driving pressure gradient is much larger than the driving force due to capillary pressure, allows the definition of a sharp front separating the fully saturated porous medium from the uninfiltrated portion.

Our attention is focused, however, on the saturated region, assuming that the uninfiltrated porous material is rigid, as occurs for some synthetic sponges. The coupled problem obtained considering a porous material deformable both when dry and when wet is currently under study (Ambrosi & Preziosi 1996).

After this introduction, the second and third sections of the present paper deal, respectively, with the formulation of the three- and the one-dimensional infiltration model, the fourth section with the formulation of the interface conditions and of the evolution equations for the boundaries delimiting the saturated region, and the fifth section with a discussion on the role of inertia and of several constitutive equations for the stress.

It is found that the resulting one-dimensional model is of Stefan type, with suitable evolution equations describing the position of the interfaces. The system of partial differential equations in the saturated porous material is hyperbolic or parabolic according to whether the inertial terms are neglected or not, and to the stress constitutive assumptions. A simulation is performed to show the importance of these terms and the applicability of the model. Finally, a comparison with an infiltration experiment made by Sommer & Mortensen (1996) is performed.

## 2. INFILTRATION MODEL

Consider the infiltration of an incompressible liquid in a deformable porous material (sometimes called sponge in this paper for brevity) made up of an incompressible solid constituent. Deformable porous media models can be deduced on the basis of the theory of mixtures (see, Atkin & Craine 1976; Bowen 1976, 1980; Rajagopal & Tao 1995; Truesdell & Toupin 1960), or by average methods, e.g. ensemble average (see Drew 1983; and Ishii 1975). A recent review of the subject with special attention to its application to composite material manufacturing has been done by Preziosi (1996).

In the absence of chemical reactions and phase changes conservation of mass of each constituent is expressed by

$$\frac{\partial \phi}{\partial t} + \nabla\cdot(\phi \mathbf{V}_S) = 0, \qquad [1]$$

$$-\frac{\partial \phi}{\partial t} + \nabla\cdot[(1-\phi)\mathbf{V}_L] = 0, \qquad [2]$$

where $\phi$ is the volume fraction of the solid constituent and $\mathbf{V}_S$ and $\mathbf{V}_L$ are, respectively, the velocity of the solid and the liquid constituent.

The momentum equations for the constituents are

$$\rho_S \phi \left( \frac{\partial \mathbf{V}_S}{\partial t} + \mathbf{V}_S \cdot \nabla \mathbf{V}_S \right) = \nabla \cdot \mathbf{T}_S + \rho_S \phi \boldsymbol{g} + \mathbf{m}^\sigma, \quad [3]$$

$$\rho_L (1 - \phi) \left( \frac{\partial \mathbf{V}_L}{\partial t} + \mathbf{V}_L \cdot \nabla \mathbf{V}_L \right) = \nabla \cdot \mathbf{T}_L + \rho_L (1 - \phi) \boldsymbol{g} - \mathbf{m}^\sigma, \quad [4]$$

where $\rho_S$ and $\rho_L$ are true density of the solid and of the liquid constituent, respectively, $\mathbf{T}_S$ and $\mathbf{T}_L$ are the so-called partial stress tensors, $\mathbf{m}^\sigma$ is the interaction force, which is related to the local interactions between the constituents across the interface separating them, and $\boldsymbol{g}$ is the gravitational acceleration.

The main difficulty in using [3], [4] is in formulating and validating the constitutive relations for the interfacial force $\mathbf{m}^\sigma$ and the partial stresses $\mathbf{T}_S$ and $\mathbf{T}_L$ appearing in them, since they cannot be measured directly. However, adding them gives

$$\rho_c \left( \frac{\partial \mathbf{V}_m}{\partial t} + \mathbf{V}_m \cdot \nabla \mathbf{V}_m \right) = - \nabla P_L + \nabla \cdot \mathbf{T}_m + \rho_c \boldsymbol{g}, \quad [5]$$

where $\rho_c = \phi \rho_S + (1 - \phi) \rho_L$ is the composite density, i.e. the density of the mixture considered as a whole, $\mathbf{V}_m = [\phi \rho_S \mathbf{V}_S + (1 - \phi) \rho_L \mathbf{V}_L] / \rho_c$ is the mass average velocity, $\mathbf{T}_m$ is the excess stress tensor for the mixture, and $P_L$ is the pore liquid pressure, which is constitutively undetermined as a direct consequence of the assumption that the two constituents are separately incompressible.

Equation [5] is the momentum equation one would obtain considering the wet porous material as a whole, without concern about the copresence of solid and liquid constituents in it. In particular, the constitutive equation for $\mathbf{T}_m$ can be developed from appropriate experiments on the wet material.

On the other hand, under some assumptions (namely, isotropy of $\mathbf{T}_L$, negligible contribution due to the acceleration of the liquid constituent compared, say, with the pressure gradient, linear dependence of $\mathbf{m}^\sigma$ on the velocity difference (see Bowen 1980) it is possible to deduce from [4] Darcy's law for the infiltration of liquids through deformable porous media

$$\mathbf{V}_L - \mathbf{V}_S = - \frac{1}{(1 - \phi) \mu} \mathbf{K}(\mathbf{B}) (\nabla P_L - \rho_L \boldsymbol{g}), \quad [6]$$

where $\mu$ is the liquid viscosity, $\mathbf{K}$ is the permeability tensor, and $\mathbf{B}$ is the left Cauchy–Green strain tensor for the solid.

Coherently with the assumption that the contribution due to the acceleration of the liquid constituent is negligible compared with the pressure gradient, the liquid acceleration is also dropped in [5] which then simplifies to

$$\rho_S \phi \left( \frac{\partial \mathbf{V}_S}{\partial t} + \mathbf{V}_S \cdot \nabla \mathbf{V}_S \right) = - \nabla P_L + \nabla \cdot \mathbf{T}_m + [\rho_S \phi + \rho_L (1 - \phi)] \boldsymbol{g}. \quad [7]$$

The two continuity equations [1], [2] imply that

$$\nabla \cdot \mathbf{V}_C = 0 \text{ where } \mathbf{V}_C = \phi \mathbf{V}_S + (1 - \phi) \mathbf{V}_L \quad [8]$$

is the composite velocity.

From Darcy's law [6] we can readily eliminate $\mathbf{V}_L$ from [8] to obtain

$$\nabla \cdot \left[ \mathbf{V}_S - \frac{1}{\mu} \mathbf{K}(\mathbf{B}) (\nabla P_L - \rho_L \boldsymbol{g}) \right] = 0. \quad [9]$$

The three-dimensional model is then obtained considering [1], [7] and [9].

It is worthwhile to remember explicitly that the continuity equation for the solid constituent [1] can be written in Lagrangian coordinates as

$$\det \mathbf{F} = \frac{\phi_*}{\phi} \tag{10}$$

where $\mathbf{F}$ is the deformation gradient for the solid, $\phi_*$ is the volume ratio of the undeformed reference configuration and we have used the incompressibility assumption.

## 3. THE ONE-DIMENSIONAL INFILTRATION MODEL

Assume now that the solid and the liquid constituents are placed in a vertical tube ($\boldsymbol{g} = -g\mathbf{e}_x$), that both flow and strain take place along the vertical direction $x$ and that the medium is isotropic in a plane perpendicular to this axis (such that the infiltration direction is a principal direction of the preform permeability tensor).

In this case the only non-trivial component of the strain tensor is the $\mathbf{e}_x \otimes \mathbf{e}_x$ component. In particular, defining the Lagrangian strain tensor

$$\mathbf{E} = \tfrac{1}{2}(\mathbf{B} - \mathbf{I}) = \epsilon \mathbf{e}_x \otimes \mathbf{e}_x, \tag{11}$$

it readily follows that

$$\epsilon = \frac{1}{2}(\det \mathbf{B} - 1) = \frac{1}{2}[(\det \mathbf{F})^2 - 1] = \frac{1}{2}\left(\frac{\phi_*^2}{\phi^2} - 1\right) \tag{12}$$

and that the only non-constant component of the Cauchy–Green strain tensor is

$$B_{xx} = (\det \mathbf{F})^2 = \frac{\phi_*^2}{\phi^2}, \tag{13}$$

which means that, in one-dimensional problems, the dependence of the permeability tensor $\mathbf{K}$ on $\mathbf{B}$ is equivalent to that on $\phi/\phi_*$.

The same is not true for the excess stress tensor $\mathbf{T}_m$ which refers to the whole mixture. In this case the possible dependence on the Cauchy–Green strain tensor involves not only the volume fraction (as in [13]), but also the fluid properties.

Initially the sponge is at rest and compressed at a volume ration $\phi_0(x)$. Only part of it dips into the liquid, say for $x \in [x_{B0}, x_{T0}]$, $x_{B0}$ being the position of the border of the sponge in the liquid (the other end of the sponge is held fixed), and $x_{T0}$ being the position of the liquid interface inside the sponge (see figure 1(a)). The rest is dry, i.e.

$$\begin{cases} \phi(t = 0, x) = \phi_0(x) \\ V_S(t = 0, x) = V_L(t = 0, x) = 0 \end{cases} \quad \text{for} \quad x \in [x_{B0}, x_{T0}]. \tag{14}$$

At time $t = 0$ a pressure gradient is applied between the extrema of the sponge driving the infiltration of the liquid upwards into the sponge. As time goes by, the liquid which penetrates into the sponge forms a horizontal interface $x_T(t)$. This is an air–liquid interface at the top of the liquid separating the fully saturated from the dry part of the compressed sponge. At the same time the wet sponge expands downwards into the pure liquid forming another horizontal interface $x_B(t)$. This is the bottom border of the sponge that lies within the liquid (see figure 1(b)). The infiltration model we will deal with is, of course, valid in the fully saturated region $[x_B(t), x_T(t)]$.

In doing this, capillary phenomena are simplified assuming the existence of a sharp front which divides the fully saturated porous medium from the remaining uninfiltrated portion. This assumption, often called slug-flow approximation, is valid when the applied pressure is much larger than the capillary pressure.

In our analyses we also assume that the dry sponge is stiff. In fact, there are many porous materials that are rigid when dry and soften when wet (e.g. some synthetic sponges). The case in which the sponge is not rigid is considered in Ambrosi & Preziosi (1996).

In one-dimension, [8] implies that the composite velocity $V_C$ does not depend on $x$, that is

$$\phi V_S + (1 - \phi)V_L = C(t). \quad [15]$$

Since the composite velocity is continuous across $x_B(t)$ (see Müller 1975; or Preziosi 1996), going all the way down to where there is only pure liquid, it is evident that $C(t)$ is equal to the inflow velocity.

Equation [15] and Darcy's law [6] give

$$V_S = C(t) + \frac{K(\phi)}{\mu}\left(\frac{\partial P_L}{\partial x} + \rho_L g\right), \quad [16]$$

$$V_L = C(t) - \frac{\phi}{1-\phi}\frac{K(\phi)}{\mu}\left(\frac{\partial P_L}{\partial x} + \rho_L g\right), \quad [17]$$

or

$$\frac{\partial P_L}{\partial x} = \frac{\mu}{K(\phi)}[V_S - C(t)] - \rho_L g. \quad [18]$$

The one-dimensional model then takes the following form

$$\frac{\partial \phi}{\partial t} + V_S\frac{\partial \phi}{\partial x} + \phi\frac{\partial V_S}{\partial x} = 0 \quad [19]$$

$$\rho_S\phi\left(\frac{\partial V_S}{\partial t} + V_S\frac{\partial V}{S}\partial x\right) = -\frac{\mu}{K(\phi)}[V_S - C(t)] + \frac{\partial \sigma}{\partial x} - \phi(\rho_S - \rho_L)g \quad [20]$$

for $x \in [x_B(t), x_T(t)]$, where the constitutive relation for the excess stress $\sigma$ is still to be specified.

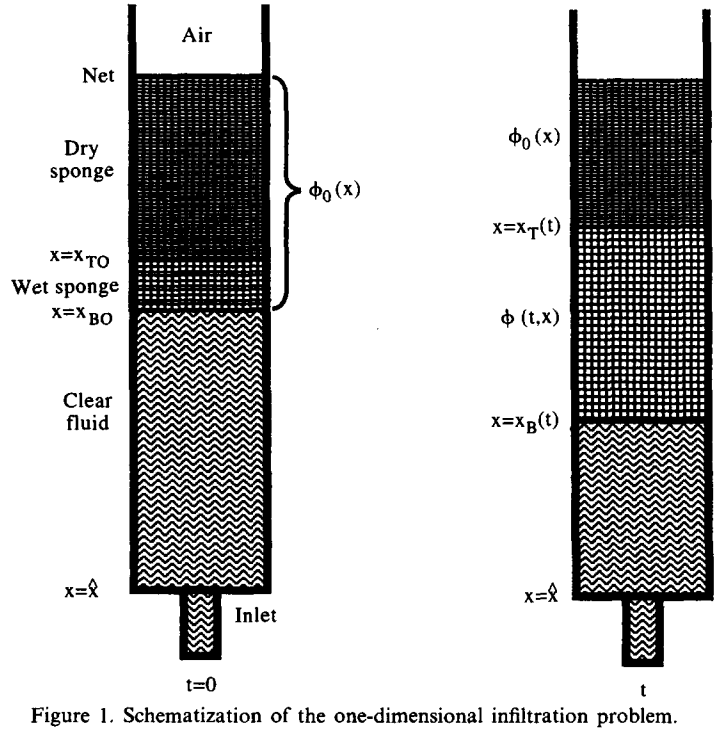


Figure 1. Schematization of the one-dimensional infiltration problem.

The quantity $C(t)$, which appears in [16]–[20] depends on how the liquid constituent is pushed into the sponge. The simplest case is when we are completely able to govern the inflow, for instance, we are able to steadily push liquid into the porous medium, which means $C(t) = \text{const.}$

A more interesting situation arises when the pressure difference

$$\Delta P_L(t) = P_L(x_B(t)) - P_L(x_T(t)) \tag{21}$$

between the top and the bottom interface is prescribed (say, constant). In setting the pressure at the top interface, for example equal to the atmospheric pressure, we assume that the gas viscosity is so small that it is easily expelled from the dry portion of the porous material, offering negligible resistance. In this case, integrating [18] we have

$$\Delta P_L(t) = C(t) \int_{x_B(t)}^{x_T(t)} \frac{\mu \, dx}{K(\phi(t, x))} - \int_{x_B(t)}^{x_T(t)} \frac{\mu V_S(t, x)}{K(\phi(t, x))} dx + \rho_L g[x_T(t) - x_B(t)], \tag{22}$$

or

$$C(t) = \frac{\frac{1}{\mu}\{\Delta P_L(t) - \rho_L g[x_T(t) - x_B(t)]\} + \int_{x_B(t)}^{x_T(t)} \frac{V_S(t, x)}{K(\phi(t, x))} dx}{\int_{x_B(t)}^{x_T(t)} \frac{dx}{K(\phi(t, x))}}. \tag{23}$$

## 4. EVOLUTION OF THE INTERFACES AND INTERFACE CONDITIONS

The system of equations [19], [20] has to be integrated in the time-varying domain $[x_B(t), x_T(t)]$. We have then to determine the evolution equations for $x_B(t)$ and $x_T(t)$ and to join to [19], [20] proper interface conditions on $\phi$ and $V_S$.

The bottom interface $x_B(t)$ is a material interface for the porous medium and therefore it has to move with the velocity of the porous medium at the bottom interface

$$\frac{dx_B}{dt}(t) = V_S(t, x_B(t)). \tag{24}$$

Similarly, the top interface $x_T(t)$ is a material interface for the liquid and, therefore, it has to move with the velocity of the liquid at the top interface

$$\frac{dx_T}{dt}(t) = V_L(t, x_T(t)). \tag{25}$$

However, the composite velocity is constant throughout the sponge and has to be continuous across $x_T(t)$ (see Müller 1975; or Preziosi 1996). If the dry porous material is assumed to be rigid, then evaluating [15] on both sides of the top interface $x_T(t)$ gives

$$C(t) = \phi(t, x_T(t))V_S(t, x_T(t)) + [1 - \phi(t, x_T(t))]V_L(t, x_T(t)) = [1 - \phi_0(x_T(t))]V_L(t, x_T(t)). \tag{26}$$

This allows to rewrite [25] as

$$\frac{dx_T}{dt}(t) = \frac{C(t)}{1 - \phi_0(x_T(t))}, \tag{27}$$

and to deduce the boundary condition

$$V_S(t, x_T(t)) = \frac{\phi(t, x_T(t)) - \phi_0(x_T(t))}{\phi(t, x_T(t))[1 - \phi_0(x_T(t))]} C(t). \tag{28}$$

The other boundary condition is the stress-free condition at the bottom interface

$$\sigma(t, x_B(t)) = 0. \tag{29}$$

It is worthwhile to observe explicitly that the time derivative of the total solid mass wet by the liquid is

$$\frac{\mathrm{d}}{\mathrm{d}t}\int_{x_B(t)}^{x_T(t)} \phi(t,x)\,\mathrm{d}x = \phi(t,x_T(t))\left[\frac{\mathrm{d}x_T}{\mathrm{d}t} - V_S(t,x_T(t))\right] = \frac{\phi_0(x_T(t))}{1-\phi_0(x_T(t))}\,C(t). \qquad [30]$$

This relation is useful to control the computational error made in the numerical integration. In particular, if $C(t) = 0$, then the total solid mass wet by the liquid is conserved. This is a direct consequence of the stiffness assumption on the dry sponge.

## 5. THE ROLE OF INERTIA AND OF THE STRESS CONSTITUTIVE EQUATION

In consolidation theory and in all fields of application of deformable porous media models, the inertia of the solid constituent is often neglected. Even when inertial terms are retained in the derivation of the model (see, for instance, Scott & Stevenson 1986; Spiegelman 1993a; Kenyon 1976; and Mow *et al.* 1984), they are eventually neglected in the applications.

This approximation is equivalent to saying that the stress in the solid and the pressure exerted by the liquid balance each other, setting each solid element in equilibrium (in this section gravity is neglected for sake of simplicity). In fact, in this case, the momentum equation [5] takes the form of a stress equilibrium equation

$$\frac{\partial \sigma}{\partial x} = \frac{\partial P_L}{\partial x}. \qquad [31]$$

The velocity of the liquid and of the solid constituents are then determined by the joined action of Darcy's law and of the conservation equation [15]. In fact, in [16], [17] the pressure gradient is functionally related to the volume ratio through [31] and the constitutive relation, that is a change in liquid pressure readily determines a change of volume ratio. The change in volume fraction and pressure gradient will then determine a change in the relative flow of the liquid with respect to the solid preform, which has to be such that the composite velocity is $x$-independent.

In this conceptual schematization of events one excludes the situation whereby the solid preform can be deformed by the direct action of the change of the liquid pressure gradient, assuming that the pressure gradient is entirely absorbed as stress in the solid preform. Keeping, instead, the inertial term of the solid constituent allows the non-equilibrium between stress in the solid element and liquid pressure acting on it to influence directly the evolution of the wet porous medium. This can be a non-negligible effect, as for example in composite manufacturing by infiltration and in some bio-mechanical problems.

In this section attention is focused on the effects of the assumptions made on the relative importance of the inertial term and on the form of the stress constitutive relation. It is shown that, as a consequence of these assumptions, the model possesses different mathematical characteristics and that inertial terms are important at early times, where the meaning of early depends on the physical parameters and on the constitutive assumptions. This section concludes with a description of a simulation that was performed to quantify these effects.

The main difficulty in dealing with deformable porous media, however, is not in treating the inertial term, but in correctly formulating the stress constitutive relation for the wet material as a whole. This is due to the fact that at the present time there are not enough experimental results available to guide the choice of one constitutive relation over another, but only general measurement of the viscoelastic properties of the constituents and observation of viscoelastic behavior of the wet material (see, Chan & Hwang 1993; Han *et al.* 1993a, b; Kendall & Rudd 1994; Kim *et al.* 1991; Parker *et al.* 1987; Patel *et al.* 1993; Rudd *et al.* 1990, 1992; Sommer & Mortensen 1996; Trevino *et al.* 1991; Young *et al.* 1991b).

In fact, despite recognizing the importance of viscoelastic effects, most papers perform or report on measurements of the stress–strain relation in uni-axial compression tests in the equilibrium condition

$$\sigma = \sigma(\epsilon), \qquad [32]$$

ruling out any viscoelastic effect. This corresponds to neglecting the effect due to the presence of the liquid matrix in the pores and to approximating the wet sponge as an elastic material.

In reality, the solid preform and the liquid matrix cannot deform independently but have to carry the load by joint deformation. This, however, does not require adding two constitutive equations, one for each constituent, since

$$\mathbf{T}_m = \phi \mathbf{T}_S + (1 - \phi)\mathbf{T}_L - \langle \rho(\mathbf{V} - \mathbf{V}_m) \otimes (\mathbf{V} - \mathbf{V}_m) \rangle, \tag{33}$$

where the last term is an averaged interaction term which is hard to model (see, for instance, Drew 1983; Ishii 1975; Preziosi 1996). It is convenient, therefore, to look directly for a constitutive relation for the wet material as a whole which possesses the characteristics exhibited by experimental observations.

The viscoelastic behavior of composite materials in their final solid form has been experimentally studied by many authors (see, for instance, Christensen 1979; Cook 1977; Gibson 1994; Isayev 1987; Macosko 1989; Mallick 1988, and references therein). But in modelling the infiltration of a deformable medium it is necessary to know the stress–strain functional relationship when the matrix material is still in its liquid form. This piece of information is lacking for the materials usually used in composite manufacturing. The only paper we found that gives quantitative data of the stress relaxation of a mixture is the one by Kim, *et al.* (1991).

Some more information can be obtained looking at similar studies dealing with the viscoelastic properties of articular cartilages (see, for instance, Holmes 1986; Holmes & Mow 1990; Kwan *et al.* 1990; Lai *et al.* 1981; Mow *et al.* 1979, 1980, 1984). In fact, the human body itself can be divided into several subsystems that can be schematized as deformable porous media permeated by organic liquids (articular cartilages, arteries, lungs, liver, kidneys, muscles, cornea, heart, brain, subcutaneous layer, and what is generally called in biomathematics soft tissue). Of course, in describing these systems osmotic effects should also be included. However, these studies show experimental evidences for the need to model the mixture at least as a Voigt–Kelvin solid

$$\mathbf{T}_m = \eta \left( \lambda_E \frac{\mathscr{D}\mathbf{E}}{\mathscr{D}t} + \mathbf{E} \right), \tag{34}$$

or as an anelastic solid

$$\lambda_T \frac{\mathscr{D}\mathbf{T}_m}{\mathscr{D}t} + \mathbf{T}_m = \eta \left( \lambda_E \frac{\mathscr{D}\mathbf{E}}{\mathscr{D}t} + \mathbf{E} \right), \tag{35}$$

where

$$\frac{\mathscr{D}\mathbf{M}}{\mathscr{D}t} = \frac{\partial \mathbf{M}}{\partial t} + \mathbf{V}_m \cdot \nabla \mathbf{M} - \mathbf{W}\mathbf{M} + \mathbf{M}\mathbf{W} - a(\mathbf{D}\mathbf{M} + \mathbf{M}\mathbf{D}) \tag{36}$$

is the convective derivative, **D** and **W** are the symmetric and antisymmetric part of the mass average velocity gradient and $a$ is a parameter ranging between $-1$ and 1 (see, for instance, Joseph 1990).

The fact that the convective derivative is based on the mass average velocity is related to the fact that the constitutive equation refers to the momentum equation of the mixture as a whole, without distinguishing macroscopically its components.

The constitutive equation [34] is not the only or the most general one that might be tried for our wet sponge. However, three parameter models are commonly used for viscoelastic fluids and solids (see Flügge 1975; Freudenthal 1966; Joseph 1990). Rheometrical methods for measuring the parameters are well known. Experiments are required in this direction in order to open a proper discussion. For instance, we think it could be useful to perform dynamical tests aimed at evaluating the response of the wet sponge compressed at different volume ratios to oscillatory twist and compression.

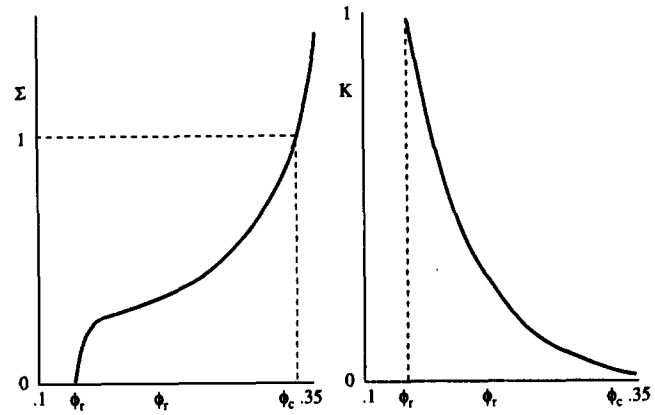


Figure 2. Behavior of the dimensionless (a) stress $\Sigma(\phi)/\Sigma(\phi_c)$ and (b) permeability $K(\phi)/K(\phi_r)$ as a function of the volume ratio. In the simulation $\phi_r = 0.135175$, $\phi_c = 1/3$, $\Sigma(\phi_c) = 9.7076 \times 10^4$ Pa and $K(\phi_r) = 1.685 \times 10^{-11}$ m$^2$.

It is useful to recall explicitly that in one dimension, strain and volume ratios are related through [12] and that measurements usually give the stress–volume ratio relation with the stress taken positive in compression, i.e.

$$\sigma = -\Sigma(\phi), \quad \text{with} \quad \Sigma'(\phi) = \frac{d\Sigma}{d\phi} > 0 \tag{37}$$

where

$$\Sigma(\phi) = -\sigma\left(\frac{1}{2}\left(\frac{\phi_*^2}{\phi^2} - 1\right)\right) = -\sigma(\epsilon), \tag{38}$$

(see figure 2(a)).

In one dimension we can then write

$$\frac{\mathscr{D}\epsilon}{\mathscr{D}t} = \frac{\partial\epsilon}{\partial t} + V_m\frac{\partial\epsilon}{\partial x} - 2a\epsilon\frac{\partial V_m}{\partial x} = -\frac{\phi_*^2}{\phi^3}\left[\frac{\partial\phi}{\partial t} + V_m\frac{\partial\phi}{\partial x} - a\phi\left(\frac{\phi^2}{\phi_*^2} - 1\right)\frac{\partial V_m}{\partial x}\right]$$

$$= -\frac{\phi_*^2}{\phi^3}\left[(V_m - V_S)\frac{\partial\phi}{\partial x} - a\phi\left(\frac{\phi^2}{\phi_*^2} - 1\right)\frac{\partial V_m}{\partial x}\right] \tag{39}$$

where we have used [12] and the continuity equation [19]. Using [15], we can express $V_m$ as

$$\rho_c V_m = (\rho_S - \rho_L)\phi V_S + \rho_L C(t). \tag{40}$$

In our one-dimensional mixture model we allow the parameters in the constitutive equation to depend on the material parameters of the fluid and the solid constituents and on the strain, as occurs for models of White–Metzner type. This is done in order to be consistent with the nonlinear elastic setting commonly described in steady compression tests.

Taking into account [39] the constitutive relation for one-dimensional deformations of an anelastic solid (see [35]) can then be written as

$$\lambda_\sigma(\phi, \mu)\left(\frac{\partial\sigma}{\partial t} + V_m\frac{\partial\sigma}{\partial x} - 2a\sigma\frac{\partial V_m}{\partial x}\right) + \sigma$$

$$= -\Sigma(\phi, \mu)\left\{\frac{2\lambda_\phi(\phi, \mu)}{\phi\left(\frac{\phi^2}{\phi_*^2} - 1\right)}\left[(V_m - V_S)\frac{\partial\phi}{\partial x} - \phi\frac{\partial V_S}{\partial x} - a\phi\left(\frac{\phi^2}{\phi_*^2} - 1\right)\frac{\partial V_m}{\partial x}\right] + 1\right\}, \tag{41}$$

while that of a Voigt–Kelvin solid (see [34]) as

$$\sigma = -\Sigma(\phi,\mu)\left\{\frac{2\lambda_\phi(\phi,\mu)}{\phi\left(\frac{\phi^2}{\phi_*^2}-1\right)}\left[(V_m - V_S)\frac{\partial\phi}{\partial x} - \phi\frac{\partial V_S}{\partial x} - a\phi\left(\frac{\phi^2}{\phi_*^2}-1\right)\frac{\partial V_m}{\partial x}\right] + 1\right\}. \quad [42]$$

Going back to the evolution equation, if inertia is neglected, then the system of equations [19], [20] can be reduced to the single equation

$$\frac{\partial\phi}{\partial t} + C(t)\frac{\partial\phi}{\partial x} + \frac{1}{\mu}\frac{\partial}{\partial x}\left(K(\phi)\phi\frac{\partial\sigma}{\partial x}\right) = 0 \quad [43]$$

where we have neglected gravity for sake of simplicity.

Assuming that the mixture behaves like an elastic material implies joining the constitutive relation [37] to [43] which yields the nonlinear convection–diffusion equation

$$\frac{\partial\phi}{\partial t} + C(t)\frac{\partial\phi}{\partial x} = \frac{1}{\mu}\frac{\partial}{\partial x}\left(K(\phi)\phi\Sigma'(\phi)\frac{\partial\phi}{\partial x}\right). \quad [44]$$

If the mixture is modelled as an anelastic solid using [41], or as a Voigt–Kelvin solid using [42], we have a model which is still parabolic, but with a structure which presents similarities to the KdV equation and to the models obtained studying magma mechanics (Fowler 1985; Richter & McKenzie 1984; Scott *et al.* 1984, 1986, 1988; Spiegelman 1993a, b). We remind that these models admit solutions for finite-amplitude solitary waves of permanent form and constant velocity, which thus might also be allowed by the present model. In this case, in analogy with what occurs in fluidized beds, one could talk of void waves in deformable porous media.

If, instead, the inertia of the solid constituent is not neglected and the mixture is modelled as an elastic material, then the resulting model

$$\begin{cases} \dfrac{\partial\phi}{\partial t} + V_S\dfrac{\partial\phi}{\partial x} + \phi\dfrac{\partial V_S}{\partial x} = 0 \\ \rho_S\phi\left(\dfrac{\partial V_S}{\partial t} + V_S\dfrac{\partial V_S}{\partial x}\right) + \Sigma'(\phi)\dfrac{\partial\phi}{\partial x} + \dfrac{\mu}{K(\phi)}[V_S - C(t)] = 0 \end{cases} \quad [45]$$

is hyperbolic. The same is also true if an anelastic constitutive equation is combined with [19], [20].

In the simulation which follows we integrate the different models considered above under the same physical situation but for different values of the parameters to analyze the differences between the results. In order to do that it is convenient to introduce dimensionless variables by scaling lengths, time and velocities by the characteristic length $x_{T0} - x_{B0}$, time $[\mu(x_{T0} - x_{B0})^2]/K_r\Sigma_c$, and velocity $K_r\Sigma_c/[\mu(x_{T0} - x_{B0})]$ where $K_r = K(\phi_r)$ is the permeability of the relaxed sponge (i.e. $\phi_r$ is such that $\Sigma(\phi_r) = 0$) and $\Sigma_c = \Sigma(\phi_c)$ is the stress of the sponge at a given volume ratio $\phi_c$, say $\phi_c = \phi_0(x_{T0})$.

In this way the momentum equation becomes

$$\mathscr{P}\phi\left(\frac{\partial V_S}{\partial t} + V_S\frac{\partial V_S}{\partial x}\right) = -\frac{1}{\tilde{K}(\phi)}[V_S - \tilde{C}(t)] + \frac{\partial\tilde{\sigma}}{\partial x}, \quad [46]$$

where

$$\mathscr{P} = \rho_S\Sigma_c\left[\frac{K_r}{\mu(x_{T0} - x_{B0})}\right]^2 \quad [47]$$

is a dimensionless parameter which gives a measure of the relative importance of the inertial term.

All variables in [46] are now dimensionless. In particular, $\tilde{K}(\phi) = K(\phi)/K(\phi_r)$, $\tilde{\sigma} = \sigma/\Sigma(\phi_c)$, and the dimensionless inflow velocity $\tilde{C}(t)$ is either given or determined by the dimensionless form of [23]

$$\tilde{C}(t) = \frac{\dfrac{\Delta P_L(t)}{\Sigma_c} + \displaystyle\int_{x_B(t)}^{x_T(t)} \frac{V_S(t,x)}{\tilde{K}(\phi(t,x))}\,dx}{\displaystyle\int_{x_B(t)}^{x_T(t)} \frac{dx}{\tilde{K}(\phi(t,x))}}, \qquad [48]$$

if the pressure drop $\Delta P_L$ between the sponge extrema is given.

The dimensionless form of the remaining equations is formally unchanged. The initial-boundary value problem is, then formed by [19] and [46] joined with one of the constitutive equations [37], [41], or [42], with the evolution equations for the boundaries [24], [27] and the boundary conditions [28], [29].

Furthermore, it is assumed that the sponge is initially at rest and compressed as a solid volume fraction

$$\phi = \begin{cases} \phi_r + (\phi_c - \phi_r)\dfrac{\tanh nx}{\tanh n} & 0 \leqslant x \leqslant 1 \\ \phi_c & x > 1 \end{cases} \qquad [49]$$

with $n = 10$, $\phi_c = 1/3$, and where $\phi_r$ is the volume ratio of the relaxed state, i.e. $\Sigma(\phi_r) = 0$.

In performing the simulation we used the data relative to the polyurethane sponge used in the experiments made by Sommer & Mortensen (1996).

The value of $\mathscr{P}$ depends strongly on the initial length of the wet sponge. For the polyurethane sponge we are considering it can reach values of order one for millimeter-sized specimens. Still higher values can be achieved in composite manufacturing since the solid preforms used in applications have higher densities, permeabilities and stresses.

Figures 3–6 present computations which bring into focus various special effects associated with inertia and different constitutive equations. In order to illustrate the effect of the inertial and of the viscoelastic terms we first consider in figures 3 and 4 the case of spontaneous relaxation of an initially compressed sponge immersed in the pure liquid with no pressure gradient forcing the infiltration process, i.e. $C(t) = 0$.

Figure 3 shows the evolution of the sponge assuming that the wet sponge behaves like an elastic material. In figure 3(a) inertia is neglected, while figure 3(b) and (c) give the evolution of the volume fraction vs $x$ at different times when inertia is considered. We remind that the model is parabolic in the former case, and hyperbolic in the latter case. The hyperbolic character can be easily identified when the continuous evolution of the system is looked at directly on the computer screen and is more pronounced at higher $\mathscr{P}$. One can actually notice that the relaxed state propagates into the sponge. The propagation of condensation–rarefaction waves may lead, especially at higher $\mathscr{P}$ and early times, to the development of regions near the border of the sponge $x = x_B(t)$ with volume ratio smaller than the one corresponding to the relaxed state (that is, $\phi < \phi_r$). From a practical point of view this is an undesirable effect for those fibrous materials which are particularly fragile to expansions. This over-relaxation of the sponge can be already identified in figure 3(b), (c) in spite of the fact that the numerical integration starts from a smooth initial condition.

Figure 4 shows the evolution with inertia considered and assuming that the wet sponge behaves like a Voigt–Kelvin solid with $\lambda_\phi = 0.1$. The higher $\lambda_\phi$ is the smoother the evolution is. In particular, it inhibits over-relaxation. The effect of the additional term in the constitutive equation is felt for times at most one order of magnitude larger than $\lambda_\phi$.

Figure 5 presents results of a simulation of the infiltration into the dry sponge compressed at a constant volume ratio $\phi_c = 1/3$ due to a constant pressure difference $\Delta P = P(x_B) - P(x_T) = \Sigma(\phi_c)$. The pressure difference pushes liquid into the sponge, so that the front $x = x_T$ dividing the wet sponge from the dry sponge advances. At the same time the other front relaxes into the liquid.

At early times the filtration of the fluid into the sponge may cause over-compression of the sponge near $x = x_T$ (i.e. regions with volume ratio $\phi > \phi_c$), because the permeability there is much smaller (remember that the dry sponge is assumed to be stiff, otherwise this over-compression would compress further the dry sponge). This is not evident in figure 5 because of the time scale but is put in evidence in figure 6(a). This effect is more pronounced for larger values of the inertial parameter $\mathscr{P}$ and less pronounced if $\lambda_\phi \neq 0$ as is shown in figure 6(b). The introduction of a non-vanishing $\lambda_\phi$ gives little differences at longer times.

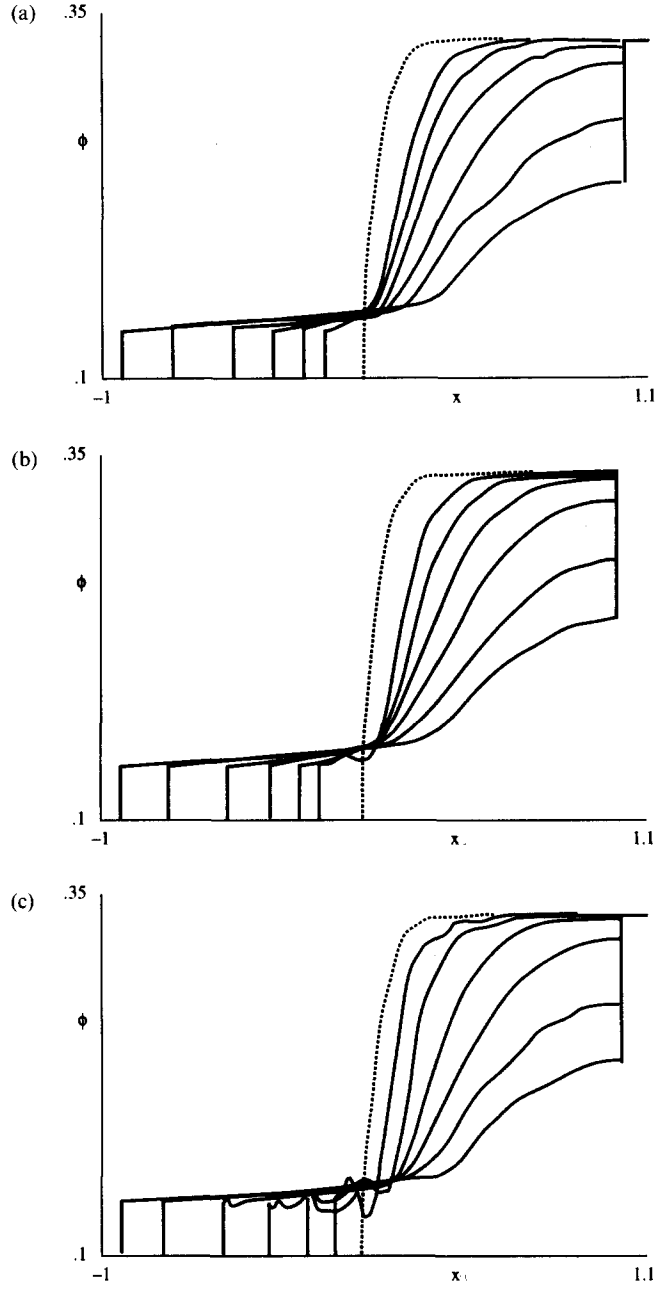


Figure 3. Spontaneous relaxation of a wet compressed elastic sponge. The fully relaxed sponge has a solid fraction $\phi_r = 0.135175$ (see figure 2(a)). The dry sponge ($x > 1$) is compressed at a volume fraction $\phi_c = 1/3$. Referring to [46], $\mathscr{P} > 0$ gives rise to hyperbolic propagation, whereas $\mathscr{P} = 0$ gives rise to a nonlinear diffusion equation (see [44]) with a characteristic monotone relaxation as shown in (a). Larger values of $\mathscr{P}$ give rise to wave propagation, and over-relaxation ($\phi < \phi_r$) as is evident in (b) and (c) which correspond, respectively, to $\mathscr{P} = 0.1$ and $\mathscr{P} = 1$. The solid volume fraction is plotted vs $x$ at different times $t = 0.1, 0.2, 0.4, 0.8, 1.6, 2.4$. The dotted line represents the initial condition.

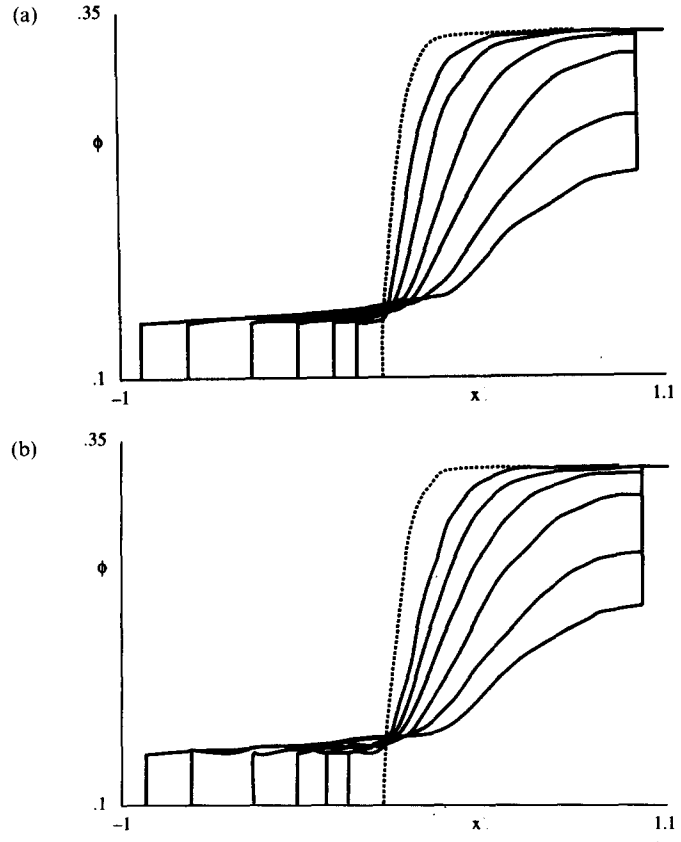


Figure 4. Spontaneous relaxation of a wet compressed Voigt–Kelvin sponge, i.e. [19, 20] combined with [42] with $\lambda_\phi = 0.1$. The fully relaxed sponge has a solid fraction $\phi_r = 0.135175$ (see figure 2(a)). The dry sponge ($x > 1$) is compressed at a volume fraction $\phi_c = 1/3$. The coefficient of the inertial term in [46] is $\mathscr{P} = 0.1$ in (a) and $\mathscr{P} = 1$ in (b). Higher values of $\lambda_\phi$ correspond to a larger dissipation which has the effect of smoothing the oscillations which arise for the elastic sponge. The solid volume fraction is plotted vs $x$ at different times $t = 0.1$, 0.2, 0.4, 0.8, 1.6, 2.4. The dotted line represents the initial condition.

Finally, in figure 7 we present a comparison with some experimental data obtained by Sommer & Mortensen (1996) who performed an infiltration experiment in a dry sponge-like material which has some similarities with our problem. Their experimental setting, however, is not fully consistent with our assumptions, and therefore the comparison can only be qualitative. In fact,

(1) Their dry sponge is not stiff, and in fact it appears to relax as time goes by.
(2) Their infiltration experiment is nearly unidirectional because of the presence of "lateral strain experienced by the porous medium (which therefore) is associated with finite velocities in $y$ and $z$ directions" (from Sommer & Mortensen 1996).
(3) It is hard from their data to identify the initial conditions, which, however will not have $V_S(t = 0, x) = 0$.

Our parameters depends crucially on the initial width $x_{T0} - x_{B0}$ of the wet sponge. We identified this by considering the moment at which the bottom border of the sponge has zero velocity, which occurs at $t \approx 5$ s and assume that this is true for all $x$, which is not strictly true. In this instant the width of the wet sponge appears to be about 4 cm.

Our results also depend on $\phi_0(x)$, which cannot be obtained from their data.

In order to compare our numerical results with the just mentioned experimental data we need introduce the dimensionless variable

$$\eta = \frac{x - x_B(t)}{x_T(t) - x_B(t)} \qquad [50]$$

which maps the interval $[x_B(t), x_T(t)]$ into the fixed interval [0, 1].

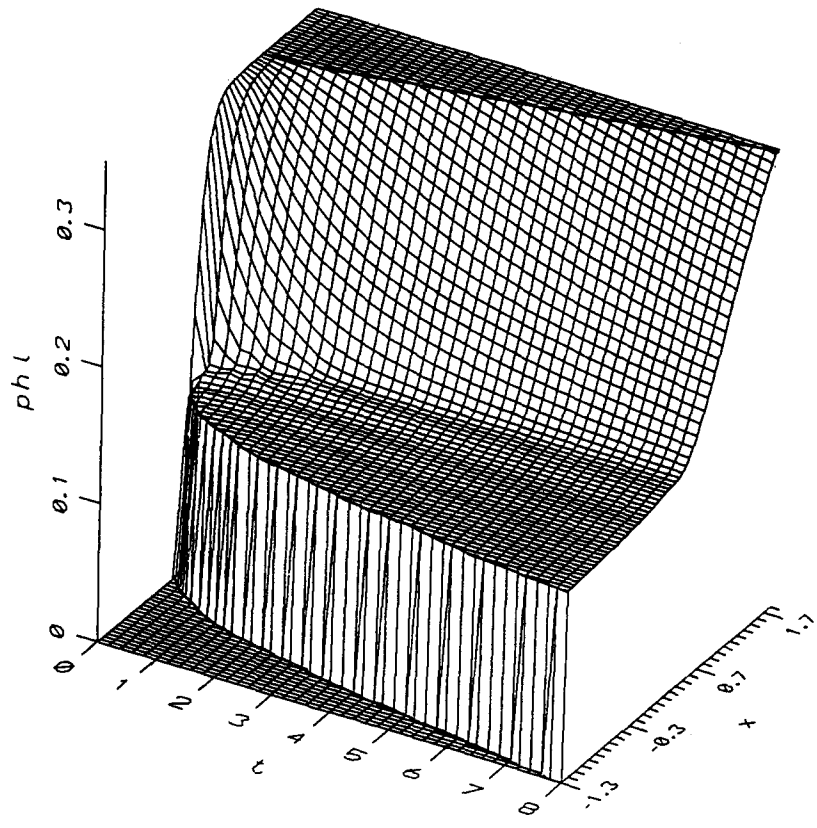


Figure 5. Infiltration in a sponge compressed at a constant volume ratio $\phi_c = 1/3$ due to a pressure difference $P(x_B) - P(x_T) = \Sigma(\phi_c)$. The front $x = x_B(t)$, i.e. the border of the wet sponge, travels to the left, while the infiltration front $x = x_T(t)$ dividing the wet sponge from the dry sponge travels to the right.

We compared our numerical results only with the experimental data they measure after 17 and 31 (which correspond to our 12 and 26 s because of our defining the initial condition after 5 s), since for later times the relaxation of the dry sponge appears to influence the experimental data.

We observed that the initial condition $\phi_0(x)$ strongly influences the evolution of the interfaces $x_B(t)$ and $x_T(t)$, but when the interval is mapped onto [0, 1] the solution for $t > 15$ s appears to be insensitive to variation in $\phi_0(x)$. Taking into account the differences between Sommer and Mortensen's and our set up, the comparison can be considered satisfactory.

The simulation presented above gives an indication of possible scenarios; but in order to perform a more detailed simulation it is necessary to have more data on the properties of the wet sponge. Once this is available we can use the modelling procedure presented here to develop a systematic simulation of the technological problem.

## 6. CONCLUSIONS

In this paper we have presented a model which can be applied to those industrial processes involving flow through sponge-like materials and, in particular, to some processes used to fabricate composite materials.

The coupled flow/deformation problem is considered in detail, which is fundamental in some of the processes mentioned above. The sensitivity of the model to the assumption made on the importance of the inertial term and on the constitutive relation is examined and shown to have significant dependence on both. For instance, elastic constitutive models may lead to over-relaxation near the sponge border, and wave propagation, while Voigt–Kelvin constitutive models have a smoothing effect. A proper discussion can be opened when the results of dynamical tests on wet sponge-like materials are available.

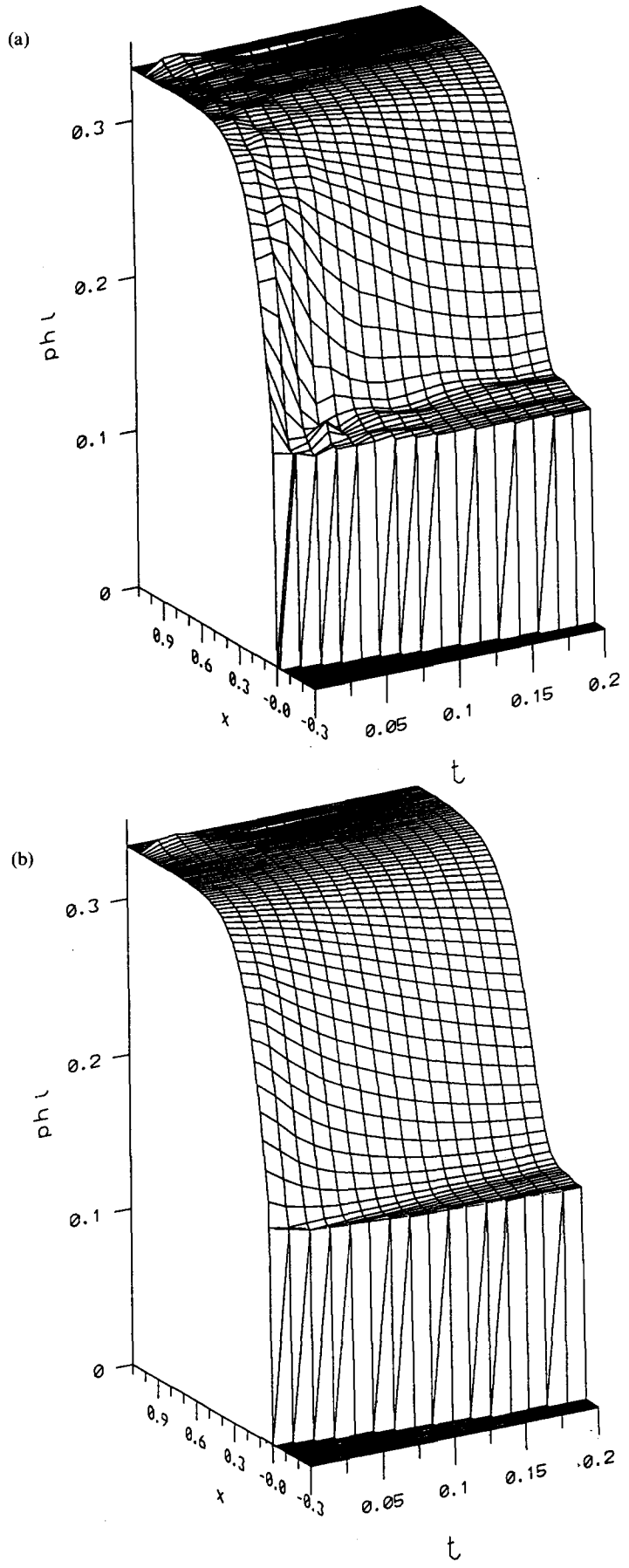


Figure 6. Blow up of figure 5 to show over-compression ($\phi > \phi_c$) of the sponge near $x = x_T(t)$ at early times. Over-relaxation ($\phi < \phi_r$) is also present (but not so evident) in (a) which corresponds to $\mathscr{P} = 0.1$, $\lambda_\phi = 0$. In (b) $\mathscr{P} = 0.1$, $\lambda_\phi = 0.1$. Over-compression is smoothed out and over-relaxation does not occur.

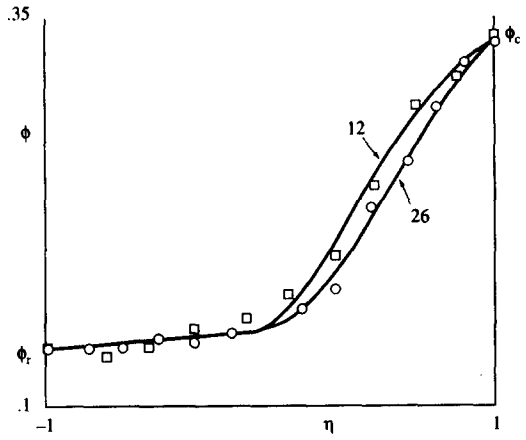


Figure 7. Comparison of numerical results with experimental data obtained by Sommer & Mortensen (1996). The interval $[x_B(t), x_T(t)]$ is linearly mapped onto [0, 1] through [50]. The results obtained for $t = 12$ and 26 s are in good agreement with the experimental data measured at $t = 17$ s (squares) and $t = 31$ s (circles). Remember that our simulation starts about 5 s after Sommer & Mortensen (1996) record their data.

The model is then applied to the case in which a liquid is pushed through a dry porous material which requires the determination of the evolution equations determining the position of the borders of the fully infiltrated region and the relative interface condition.

Finally, a comparison with a similar experiments done by Sommer & Mortensen (1996) is performed yielding a satisfactory agreement.

*Acknowledgements*—L. Preziosi is grateful to the Minnesota Supercomputer Institute, the National Research Council, and to the Italian Ministry for the University and Scientific Research for funding the present research and wishes to thank the Department of Aerospace Engineering and Mechanics of the University of Minnesota for the kind hospitality. The work of D. D. Joseph and G. S. Beavers was supported in part by the NSF (CBTE), the ARO (Mathematics) and the DOE (Office of Basic Energy Sciences).

## REFERENCES

Ambrosi, D. & Preziosi, L. 1996 Modelling matrix injection through deformable porous preforms. *Composites*, Special Issue of the Fourth Intnl Conf. on Flow Processes in Composite Materials (Edited by J. Goshawk) (to appear).

Atkin, R. J. & Craine, R. E. 1976 Continuum theories of mixtures: basic theory and hystorical development. *Quart. J. Mech. Appl. Math.* **29,** 209–244.

Barenblatt, G. I., Entov, V. M. & Ryzhik, V. M. 1990 *Theory of Fluid Flows through Natural Rocks*. Kluwer, Dordrecht.

Barry, S. & Aldis, G. K. 1991 Unsteady flow induced deformation of porous materials. *Int. J. Nonlinear Mech.* **26,** 687–699.

Bear, J. & Bachmat, Y. 1990 *Introduction to Modeling of Transport Phenomena in Porous Media*. Kluwer, Dordrecht.

Bowen, R. M. 1976 Theory of mixtures. In *Continuum Mechanics* (Edited by Eringen, A. C.), Vol. 3. Academic Press, New York.

Bowen, R. M. 1980 Incompressible porous media models by use of the theory of mixtures. *Int. J. Engng Sci.* **18,** 1129–1148.

Chan, A. W. & Hwang, S. T. 1993 Modeling resin transfer molding of polyimide (PMR-15)/fiber composites. *Polymer Compos.* **14,** 524–528.

Christensen, R. M. 1979 *Mechanics of Composite Materials*. Wiley, Chichester.

Cook, J. P. 1977 *Composite Construction Methods*. Wiley, Chichester.

Drew, D. 1983 Mathematical modeling of two-phase flow. *Ann. Rev. Fluid Mech.* **15,** 261–291.

Fasano, A., Primicerio, M. & Baldini, G. 1992 Mathematical models for espresso coffee

preparation. In *Proc. 6th European Conf. Math. Ind.* (Edited by Hodnett, F.), pp. 137–140. Teubner, Stuttgard.

Fasano, A. & Primicerio, M. 1993 Mathematical models for filtration through porous media interacting with the flow. *Nonlinear Math. Problems in Industry* **1,** 61–85.

Flügge, W. 1975 *Viscoelasticity*. Springer, Berlin.

Fowler, A. 1985 A mathematical model of magma transport in the asthenosphere. *Geophys. Astrophys. Fluid Dyn.* **33,** 33–96.

Freudenthal, A. M. 1966 *Mechanics of Solids*. Wiley, Chichester.

Gibson, R. F. 1994 *Principles of Composite Material Mechanics*. McGraw-Hill, New York.

Gonzalez-Romero, V. M. & Macosko, C. W. 1990 Process parameters estimation for structural reaction injection molding and resin transfer molding. *Polym. Engng. Sci.* **30,** 142–146.

Han, K. Lee, L. J. & Liou, M. J. 1993a Fiber mat deformation in liquid composite molding. II: modeling. *Polymer Compos.* **14,** 151–160.

Han, K., Trevino, L., Lee, L. J. & Liou, M. J. 1993b Fiber mat deformation in liquid composite molding. I: experimental analysis. *Polymer Compos.* **14,** 144–150.

Holmes, M. H. & Mow, V. C. 1990 The nonlinear characteristics of soft gels and hydrated connective tissues in ultrainfiltration. *J. Biomech.* **23,** 1145–1156.

Isayev, A. I. 1987 *Injection and Compression Molding Fundamentals*. Marcel Dekker, New York.

Ishii, M. 1975 *Thermo-fluid Dynamic Theory of Two-phase Flows*. Eyrolles, Paris.

Joseph, D. D. 1990 *Fluid Dynamics of Viscoelastic Liquids*. Springer, Berlin.

Kendall, K. N. & Rudd, C. D. 1994 Flow and cure phenomena in liquid composite molding. *Polymer Comps.* **15,** 334–348.

Kenyon, D. E. 1976 Transient filtration in a porous elastic cylinder. *Appl. Mech.* **98,** 594–598.

Kenyon, D. E. 1979 A mathematical model of water flux through aortic tissue. *Bull. Math. Biol.* **41,** 79–90.

Kim, Y. R., McCarthy, S. P. & Fanucci, J. P. 1991 Compressibility and relaxation of fiber reinforcements during composite processing. *Polymer Compos.* **12,** 13–19.

Kwan, M. K., Lai, W. M. & Mow, V. C. 1990 A finite deformation theory of cartilage and other soft hydrated connective tissues: Part I—equilibrium results. *J. Biomech.* **23,** 145–155.

Lacoste, E., Aboulfatah, M., Danis, M. & Girot, F. 1993 Numerical simulation of the infiltration of fibrous preforms by a pure metal. *Metall. Trans.* **24A,** 2667–2678.

Lacoste, E., Danis, M., Girot, F. & Quennisset, J. M. 1991 Numerical simulation of the injection moulding of thin parts by liquid metal infiltration of fibrous preform. *Mater. Sci. Engng* **A135,** 45–49.

Lai, W. M., Hou, J. S. & Mow, V. C. 1990 A triphasic theory for the swelling properties of hydrated charged soft biological tissues. In *Biomechanics of Diarthroidal Joints* (Edited by Mow, V. C.), Vol. 1, pp. 283–312. Springer, Berlin.

Lai, W. M., Mow, V. C. & Roth, V. 1981 Effects of nonlinear strain-dependent permeability and rate of compression on the stress behaviour of articular cartilage. *J. Biomech. Engng* **103,** 61–66.

Lancellotta, R. 1995 *Geotechnical Engineering*. Balkema, Rotterdam.

Lee, I. K., White, W. & Ingles, O. G. 1983 *Geotechnical Engineering*. Pitman, London.

Lord, E. 1955 Air through plugs of textile fibers. *Textile Inst. Trans.* **46,** T191–T195.

Macosko, C. W. 1989 *Fundamental of Reaction Injection Molding*. Hanser, Münich.

Mallick, P. K. 1988 *Fiber-reinforced Composites: Materials, Manufacturing and Design*. Marcel Dekker, New York.

Mortensen, A. & Wong, T. 1990 Infiltration of fibrous preforms by a pure metal: Part III. Capillary phenomenon. *Metall. Trans.* **21A,** 2257–2263.

Mow V. C., Holmes M. H. & Lai, W. M. 1984 Fluid transport and mechanical problems of articular cartilage: a review. *J. Biomech.* **17,** 377–394.

Mow, V. C., Kuei, S. C., Lai, W. M. & Armstrong, C. G. 1980 Biphasic creep and stress relaxation of articular cartilage: theory and experiment. *J. Biomech. Engng* **102,** 73–84.

Mow, V. C. & Lai, W. M. 1979 Mechanics of animal joints. *Ann. Rev. Fluid Mech.* **11,** 247–288.

Müller, I. 1975 Thermodynamics of mixtures of fluids. *J. Mécanique* **14,** 267–303.

Oomens, C. W. J., Van Campen, D. H. & Grootenboer, H. J. 1987 A mixture approach to the mechanics of skin. *J. Biomech.* **20,** 877–885.

Parker, K. H., Mehta, R. V. & Caro, C. G. 1987 Steady flow in porous, elastically deformable materials. *J. Appl. Mech.* **54,** 794–800.

Patel, N., Rohatgi, V. & Lee, L. J. 1993 Influence of process and material variables on resin-fiber interface in liquid composite molding. *Polymer Compos.* **14,** 161–172.

Preziosi, L. 1996 The theory of deformable porous media and its application to composite material manufacturing. *Surveys in Mathematics for Industry* (to appear).

Rajagopal, K. R. & Tao, L. 1995 *Mechanics of Mixtures*. World Scientific, Singapore.

Richter, F. M. & McKenzie, D. 1984 Dynamical models for melt segregation from a deformable matrix. *J. Geog.* **92,** 729–740.

Rudd, C. D. & Kendall, K. N. 1992 Towards a manufacturing technology for high-volume production of composite components. *Proc. Instn Mech. Engrs* **206,** 77–91.

Rudd, C. D., Owen, M. J. & Middleton, V. 1990 Effects of process variables on cycle time during resin transfer moulding for high volume manufacture. *Mater. Sci. Techn.* **6,** 656–665.

Scott, D. 1988 The competition between percolation and circulation in a deformable porous medium. *J. Geophys. Res.* **93,** 6451–6462.

Scott, D. & Stevenson, D. 1984 Magma solitons. *Geophys. Res. Lett.* **11,** 1161–1164.

Scott, D. & Stevenson, D. 1986 Magma ascent by porous flow. *J. Geophys. Res.* **91,** 9283–9296.

Sommer, J. L. & Mortensen, A. 1996 Forced unidirectional infiltration of deformable porous media. *J. Fluid Mech.* **311,** 193–215.

Sorek, S. and Sideman, S. 1986 A porous medium approach for modelling heart mechanics. Part 1: theory. *Math. Biosci.* **81,** 1–14.

Spiegelman, M. 1993a Flow in deformable porous media: Part 1. Simple analysis. *J. Fluid Mech.* **247,** 17–38.

Spiegelman, M. 1993b Flow in deformable porous media: Part 2. Numerical analysis. *J. Fluid Mech.* **247,** 39–63.

Taub, P. A., 1967 The interaction of a fibre tangle. *J. Fluid Mech.* **27,** 561–580.

Trevino, L., Rupel, K., Young, W. B., Liou, M. J. & Lee, L. J. 1991 Analysis of resin injection molding in molds with preplaced fiber mats. I: permeability and compressibility measurements. *Polymer Compos.* **12,** 20–29.

Truesdell, C. A. & Toupin, R. A. 1960 The classical field theories. In *Handbuck der Phisik* (Edited by Flügge, S.), Vol. III/1. Springer, Berlin.

Yamauchi, T. & Nishida, Y. 1995 Infiltration kinetics of fibrous preforms by aluminum with solidification. *Acta Metall. Mater.* **43,** 1313–1321.

Young, W. B., Han, K., Fong, L. H., Lee, L. J. & Liou, M. J. 1991a Flow simulation in molds with preplaced fiber mats. *Polymer Compos.* **12,** 391–403.

Young, W. B., Rupel, K., Han, K., Lee, L. J. & Liou, M. J. 1991b Analysis of resin injection molding in molds with preplaced fiber mats. II: numerical simulation and experiments of mold filling. *Polymer Compos.* **12,** 30–38.